

Temporal non-equilibrium dynamics of a Bose Josephson junction in presence of incoherent excitations

Mauricio Trujillo-Martinez,¹ Anna Posazhennikova,^{2,*} and Johann Kroha^{1,†}

¹*Physikalisches Institut and Bethe Center for Theoretical Physics,
Universität Bonn, Nussallee, 12, D-53115 Bonn, Germany*

²*Department of Physics, Royal Holloway, University of London,
Egham, Surrey TW20 0EX, United Kingdom*

(Dated: December 1, 2014)

Abstract

The time-dependent non-equilibrium dynamics of a Bose-Einstein condensate (BEC) typically generates incoherent excitations out of the condensate due to the finite frequencies present in the time evolution. We present a detailed derivation of a general non-equilibrium Green's function technique which describes the coupled time evolution of an interacting BEC and its single-particle excitations in a trap, based on an expansion in terms of the exact eigenstates of the trap potential. We analyze the dynamics of a Bose system in a small double-well potential with initially all particles in the condensate. When the trap frequency is larger than the Josephson frequency, $\Delta > \omega_J$, the dynamics changes at a characteristic time τ_c abruptly from slow Josephson oscillations of the BEC to fast Rabi oscillations driven by quasiparticle excitations in the trap. For times $t < \tau_c$ the Josephson oscillations are undamped, in agreement with experiments. We analyze the physical origin of the finite scale τ_c as well as its dependence on the trap parameter Δ .

PACS numbers: 67.85.-d, 67.85.De, 03.75.Lm

*Email: anna.posazhennikova@rhul.ac.uk

†Email: kroha@th.physik.uni-bonn.de

I. INTRODUCTION

Time-dependent phenomena are at the heart of the physics of ultracold atomic gases and, in particular, Bose-Einstein condensates (BEC). The creation of BECs in optical traps [1, 2] has opened a box of Pandora for the study of temporal dynamics. This is because the relevant time scales in these systems allow for direct access to the time evolution, like quench dynamics [3, 4] or DC and AC Josephson oscillations [5, 6], but also because most transport experiments are done by applying time-dependent external fields, like ratchet potentials [7], or by expansion experiments [1, 2], since stationary transport cannot be driven easily in the neutral, finite-size systems.

There are several powerful numerical methods which target dynamical behaviour of superfluids. For instance, in one-dimensional systems, quench and relaxation dynamics as well as temporal spread of correlations have been treated by time-dependent density matrix renormalization group [8] and non-equilibrium dynamical mean-field theory for bosons [9]. Also the exact quantum dynamics of a 1D bosonic Josephson junction (BJJ) has been investigated by solving the many-body Schrödinger equation of motion by using the multiconfigurational time-dependent Hartree for bosons (MCTDHB) method [10]. This work demonstrated that methods based on the standard semiclassical Gross-Pitaevskii description are insufficient for capturing the complicated dynamics of the BJJ, and a many-body approach is necessary [10]. It is because a time-evolving system will always create incoherent excitations above the BEC (which we will call quasiparticle (QP) excitations), even if it was initially prepared with all particles in the BEC, provided the frequencies characterizing its time dependence are larger than the lowest QP excitation energy, characterized by the trap frequency. If the BEC is initially prepared in an excited state, for instance, by a spatial modulation of the BEC amplitude or by an occupation imbalance of a BEC in a double-well potential, QP excitations out of the condensate are necessary to thermalize the system, i.e., to reach a thermal distribution of all states and to accommodate the entropy of the thermal state. Hence, one may expect that even in a non-integrable system one can prevent thermalization by making the trap small enough, so that the trap frequency exceeds the characteristic frequency of the time evolution. Multiple undamped (non-thermalizing) [5, 11] as well as strongly damped (thermalizing) [12] Josephson oscillations of BECs in double-well potentials have been observed experimentally in traps with different sizes and

particle numbers. The above discussion exemplifies the potential necessity of considering incoherent excitations in any temporal evolution of a BEC.

A first, general description of Bose many-body systems beyond the Gross-Pitaevskii means field dynamics was developed in the seminal works by Beliaev [13], Kadanoff and Baym [14], Kane and Kadanoff [15], and Hohenberg and Martin [16]. A kinetic theory which includes collisions between then condensate and non-condensate part of the system was developed by Griffin, Nikuni and Zaremba [17]. Further approaches to a quantum kinetic description can be found in Refs. [18–20] and references therein. However, the wide applicability of these methods is somewhat hampered by the large number of variables inherent to the spatial representation, and/or (as well as in numerical methods [10]) suitability for only moderate number of atoms.

In the present paper we lay out a general, tractable method for the quantum dynamics of Bose-Einstein condensed systems in the presence of non-condensate excitations. It is based on a systematical expansion of the bosonic field operator in the eigenstates of a non-interacting Bose system in an arbitrary trap potential [21], where the operators for the lowest-lying states are replaced by their respective, time-dependent condensate amplitudes and the full quantum dynamics of the excited states is retained. We derive the coupled equations of motion for the classical condensate propagator and the quantum propagator of the excitations. By using this eigenstate representation, the spatial dependence is cast into the eigenstate wavefunctions and the number of degrees of freedom can be limited to the number of trap states to be considered, thus keeping the quantum problem tractable even for complicated trap potentials, depending only on a few system parameters. This allows us to treat any number of particles.

While our formalism is completely general, in this work we apply it to a system of an interacting Bose gas confined in a double-well potential with an initial population imbalance of the BECs in the left and in the right potential well. This system is established to exhibit Josephson oscillations [5, 6, 23].

The Josephson effect, well known from superconductors [24, 25] and superfluids [26, 27] has its peculiarities in BEC systems [23, 28–32]. Apart from already mentioned experiments it has been also observed in 1D Bose Josephson junctions on a chip [33] and arrays of Bose-Einstein condensates [34]. The BJJ is usually described in terms of the oscillating condensate

population imbalance

$$z(t) = \frac{N_1(t) - N_2(t)}{N_1(0) + N_2(0)}, \quad (1)$$

where N_1 (N_2) is the number of particles in the left (right) well. The dynamics of $z(t)$ is very sensitive to interactions. One distinguishes two regimes: a delocalized regime with the time average $\langle z(t) \rangle = 0$, and a self-trapped (ST) regime with $\langle z(t) \rangle \neq 0$ [5, 23]. The transition from the delocalized to the self-trapped regime occurs when the initial population imbalance $z(0)$ exceeds a critical value $z_c(0)$ for fixed interaction, or equivalently, the interaction strength between bosons becomes greater than a certain critical value, which depends on $z(0)$.

Once incoherent single-particle excitations are taken into account, the semiclassical dynamics of the BJJ drastically changes [10, 21, 35, 36]. First of all, the self-trapped state is destroyed by qp excitations [10, 21]. Secondly, we have shown that the non-equilibrium QP dynamics does not set in instantaneously as the Josephson coupling is switched on, but with some delay, described by a time scale τ_c [21]. For $t > \tau_c$ QPs are excited in an avalanche manner leading to fast Rabi-like oscillations of the QP occupation numbers and of the condensates between the wells. We provide a detailed analysis of the origin of τ_c and its dependence on systems parameters.

The paper is organized as follows. In Section II we define the model Hamiltonian and main parameters of the problem. In Section III we present the general formalism in terms of Keldysh Dyson equations for condensed and non-condensed particles. In Section IV we apply our formalism to a double-well potential and consider the effect of QPs on the BJJ within Bogoliubov-Hartree-Fock approximation. We discuss our results for particle imbalances, and inverse τ_c versus various system parameters in Section V. Main conclusions and perspectives are given in Section VI.

II. THE MODEL HAMILTONIAN

A system of weakly interacting bosons, trapped in an external double-well potential (Fig. 1), is most generally described by the Hamiltonian

$$H = \int d\mathbf{r} \hat{\Psi}^\dagger(\mathbf{r}, t) \left(-\frac{\nabla^2}{2m} + V_{ext}(\mathbf{r}, t) \right) \hat{\Psi}(\mathbf{r}, t) + \frac{g}{2} \int d\mathbf{r} \hat{\Psi}^\dagger(\mathbf{r}, t) \hat{\Psi}^\dagger(\mathbf{r}, t) \hat{\Psi}(\mathbf{r}, t) \hat{\Psi}(\mathbf{r}, t), \quad (2)$$

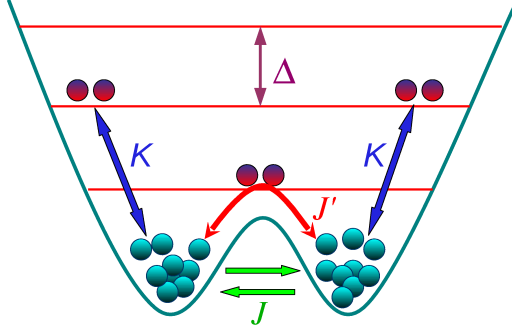


FIG. 1: Bose-Einstein condensate in a double well potential with discrete energy levels. Blue particles are condensed ones, and red particles are the particles excited out of the condensates. J is the Josephson coupling between the wells, J' is the QP-assisted Josephson coupling, K is the interaction between the QPs and the condensed particles, Δ is the interlevel splitting.

where $\hat{\Psi}(\mathbf{r}, t)$ is a bosonic field operator, and we assumed a contact interaction between the bosons with $g = 4\pi a_s/m$ (a_s is the s-wave scattering length). V_{ext} is the external double-well trapping potential.

We now expand the field operator $\hat{\Psi}(\mathbf{r}, t)$ in terms of a complete basis $\mathbb{B} = \{\varphi_-, \varphi_+, \varphi_1, \varphi_2, \dots, \varphi_M\}$ of the exact single-particle eigenstates of the double well potential $V_{ext}(\mathbf{r}, t > 0)$ after the coupling between the wells is turned on. Note that the ground state wavefunction has a zero in the barrier between the wells, thus minimizing its energy, i.e., for a symmetric double-well, it is parity antisymmetric, while the first excited state is symmetric. Hence, we denote the ground state wavefunction of the double well by φ_- , the first excited state wavefunction by φ_+ , the second excited state by φ_1 and so on. The field operator reads in the eigenbasis of the double-well potential,

$$\hat{\Psi}(\mathbf{r}, t) = \phi_1(\mathbf{r})\hat{b}_{01}(t) + \phi_2(\mathbf{r})\hat{b}_{02}(t) + \sum_{n=1}^M \varphi_n(\mathbf{r})\hat{b}_n(t), \quad (3)$$

where we have applied the transformation, $\hat{b}_{01}(t) = (\hat{b}_- + \hat{b}_+)/\sqrt{2}$, $\hat{b}_{02}(t) = (\hat{b}_- - \hat{b}_+)/\sqrt{2}$ on the operators $\hat{b}_{\pm}(t)$ for particles in the φ_{\pm} subspace, with the wavefunctions $\phi_1(\mathbf{r}) = (\varphi_-(\mathbf{r}) + \varphi_+(\mathbf{r}))/\sqrt{2}$ and $\phi_2(\mathbf{r}) = (\varphi_-(\mathbf{r}) - \varphi_+(\mathbf{r}))/\sqrt{2}$. Since the $\varphi_+(\mathbf{r})$ ($\varphi_-(\mathbf{r})$) have the same (the opposite) sign in the two wells, the $\phi_{1,2}(\mathbf{r})$ are localized in the left or right well, respectively, i.e., they approximately constitute the ground state wavefunctions of the left and right well [22]. We now perform the Bogoliubov substitution for the (approximate)

ground states in each of the two wells,

$$\hat{b}_{0\alpha}(t) \rightarrow a_\alpha(t) = \sqrt{N_\alpha(t)} e^{i\theta_\alpha(t)}, \quad (4)$$

$\alpha = 1, 2$, where N_α and θ_α are the number of particles and the phase of the condensate in the left (right) well of the potential. The field operator then reads,

$$\hat{\Psi}(\mathbf{r}, t) = \phi_1(\mathbf{r})a_1(t) + \phi_2(\mathbf{r})a_2(t) + \sum_{n=1}^M \varphi_n(\mathbf{r})\hat{b}_n(t), \quad (5)$$

The first two terms in Eq. (5) constitute the usual two-mode approximation for a condensate in a double well [23, 30, 32]. The Bogoliubov substitution neglects phase fluctuations in the ground states of each of the potential wells, while the full quantum dynamics is taken into account for the excited states, φ_n , $n = 1, 2, \dots, M$. This is justified when the BEC particle numbers are sufficiently large, $N_\alpha \gg 1$, e.g., for the experiments [5]. The applicability of the semiclassical approximation has been discussed in detail in Refs. [35–37] and has been tested experimentally in Ref. [38]. Note that Eq. (5) is a complete expansion in the single-particle eigenbasis of the double well. Therefore, one may ascribe to the low-lying excitations above the states ϕ_1, ϕ_2 the character of collective BEC excitations, while the high-energy excitations have the character of single-particle excitations, as is well-known for the case of a translationally invariant BEC [39]. In the numerical evaluations we will limit the number of levels which can be occupied by the QPs to $M = 5$.

At time $t = 0$ the barrier between the wells is suddenly lowered, and a Josephson link is established between the two condensate reservoirs. The Hamiltonian for our system for $t > 0$ is then

$$H = H_{BEC} + H_{qp} + H_{mix}. \quad (6)$$

H_{BEC} describes only condensate particles

$$H_{BEC} = E_0 \sum_{\alpha=1}^2 a_\alpha^* a_\alpha + \frac{U}{2} \sum_{\alpha=1}^2 a_\alpha^* a_\alpha^* a_\alpha a_\alpha - J(a_1^* a_2 + a_2^* a_1). \quad (7)$$

Here we consider symmetric wells with equal interparticle interactions:

$$E_0 = \int d\mathbf{r} \left[\frac{\hbar^2}{2m} |\nabla \phi_{1,2}(\mathbf{r})|^2 + \phi_{1,2}^2 V_{ext}(\mathbf{r}) \right], \quad (8)$$

$$U = g \int d\mathbf{r} |\phi_{1,2}(\mathbf{r})|^4, \quad (9)$$

and the Josephson coupling

$$J = -2 \int d\mathbf{r} \left[\frac{\hbar^2}{2m} (\nabla \phi_1 \nabla \phi_2) + \phi_1 \phi_2 V_{ext}(\mathbf{r}) \right]. \quad (10)$$

Note that there is no time dependence of V_{ext} for the times considered, $t > 0$, since the Josephson tunnelling J was turned on for times $t > 0$, and kept constant afterwards. H_{qp} corresponds to the single-particle excitations to higher levels

$$H_{qp} = \sum_{n=1}^M \epsilon_n \hat{b}_n^\dagger \hat{b}_n + \frac{U'}{2} \sum_{n,m=1}^M \sum_{l,s=1}^M \hat{b}_m^\dagger \hat{b}_n^\dagger \hat{b}_l \hat{b}_s, \quad (11)$$

where

$$\epsilon_n = \int d\mathbf{r} \varphi_n(\mathbf{r}) \left(-\frac{\nabla^2}{2m} + V_{ext}(\mathbf{r}) \right) \varphi_n(\mathbf{r}). \quad (12)$$

For computational simplicity we assume in the following that the levels are equidistant, $\epsilon_n = n\Delta$, with Δ the level spacing. This assumption does not restrict the generality of the formalism. It becomes exact, if $V_{ext}(\mathbf{r})$ is harmonic for large energies, i.e., for $V_{ext}(\mathbf{r}) \gtrsim \epsilon_1$.

U' is the repulsive interaction between single-particle excitations

$$U' = g \int d\mathbf{r} \varphi_n(\mathbf{r}) \varphi_m(\mathbf{r}) \varphi_l(\mathbf{r}) \varphi_s(\mathbf{r}). \quad (13)$$

Finally, mixing between the BECs and the system of QP excitations is described by

$$H_{mix} = \frac{1}{2} \sum_{\alpha,\beta=1}^2 \sum_{n,m=1}^M K_{\alpha\beta nm} [(a_\alpha^* a_\beta^* \hat{b}_n \hat{b}_m + h.c.) + 4a_\alpha^* a_\beta \hat{b}_n^\dagger \hat{b}_m]. \quad (14)$$

Here

$$K_{\alpha\beta nm} = g \int d\mathbf{r} \phi_\alpha(\mathbf{r}) \phi_\beta(\mathbf{r}) \varphi_n(\mathbf{r}) \varphi_m(\mathbf{r}). \quad (15)$$

It is convenient to introduce two interaction constants

$$K = 2K_{11nm} = 2K_{22nm} \quad (16)$$

$$J' = 2K_{12nm} = 2K_{21nm}, \quad (17)$$

so that terms proportional to J' describe QP-assisted Josephson tunneling. H_{mix} is then

$$\begin{aligned} H_{mix} = & J' \sum_{n,m=1}^M \left[(a_1^* a_2 + a_2^* a_1) \hat{b}_n^\dagger \hat{b}_m + \frac{1}{2} (a_1^* a_2^* \hat{b}_n \hat{b}_m + h.c.) \right] \\ & + K \sum_{\alpha=1}^2 \sum_{n,m=1}^M \left[a_\alpha^* a_\alpha \hat{b}_n^\dagger \hat{b}_m + \frac{1}{4} (a_\alpha^* a_\alpha^* \hat{b}_n \hat{b}_m + h.c.) \right]. \end{aligned} \quad (18)$$

Hereafter all our energy scales are counted from E_0 . The main parameters in our model are, hence, the interlevel spacing Δ , the QP-assisted Josephson coupling J' and the QP-BEC interaction K (Fig. 1).

In the next chapters we proceed to derive the equations of motion for the condensates and the QP excitations described by the quantum operators \hat{b}, \hat{b}^\dagger .

III. GENERAL FORMALISM

A. Quantum kinetic theory: Dyson equations and self-energies

In this section we formulate the quantum kinetic theory of the Bose Josephson junction in terms of non-equilibrium Keldysh Green's functions [41] defined along the Keldysh time contour. To shorten the notations we denote the classical part of our field operator (5) as $\Psi_0(\mathbf{r}, t)$ and the quantum part as $\tilde{\Psi}(\mathbf{r}, t)$. We define correspondingly two one-particle Green's functions, one for the QPs, \mathbf{G} , and one for the condensed particles, \mathbf{C} .

$$\mathbf{G}(1, 1') = -i \begin{pmatrix} \langle T_C \tilde{\Psi}(1) \tilde{\Psi}^\dagger(1') \rangle & \langle T_C \tilde{\Psi}(1) \tilde{\Psi}(1') \rangle \\ \langle T_C \tilde{\Psi}^\dagger(1) \tilde{\Psi}^\dagger(1') \rangle & \langle T_C \tilde{\Psi}^\dagger(1) \tilde{\Psi}(1') \rangle \end{pmatrix} = \begin{pmatrix} G(1, 1') & F(1, 1') \\ \bar{F}(1, 1') & \bar{G}(1, 1') \end{pmatrix}, \quad (19)$$

where $1 \equiv (\mathbf{r}, t)$, $1' \equiv (\mathbf{r}', t')$, and T_C denotes time ordering along the Keldysh contour, i.e. each of the bosonic Green's functions G and F will be a 2×2 matrix in Keldysh space. The condensate propagator \mathbf{C} is classical with trivial time ordering,

$$\mathbf{C}(1, 1') = -i \begin{pmatrix} \Psi_0(1) \Psi_0^*(1') & \Psi_0(1) \Psi_0(1') \\ \Psi_0^*(1) \Psi_0^*(1') & \Psi_0^*(1) \Psi_0(1') \end{pmatrix}. \quad (20)$$

For the derivation of the equation of motion for \mathbf{G} and \mathbf{C} , we proceed in the standard way (see, for instance Refs. [17, 42]). We first write down the associated Dyson equations for both Green's functions on the Keldysh contour, which read as follows,

$$\int_C d2 [\mathbf{G}_0^{-1}(1, 2) - \mathbf{S}^{HF}(1, 2)] \mathbf{C}(2, 1') = \int_C d2 \mathbf{S}(1, 2) \mathbf{C}(2, 1'), \quad (21)$$

$$\int_C d2 [\mathbf{G}_0^{-1}(1, 2) - \mathbf{\Sigma}^{HF}(1, 2)] \mathbf{G}(2, 1') = \mathbf{1} \delta(1 - 1') + \int_C d2 \mathbf{\Sigma}(1, 2) \mathbf{G}(2, 1'), \quad (22)$$

where $\int_C d2 \equiv \int d\mathbf{r}_2 \int_C dt_2$ and the subscript C denotes the time integration along the Keldysh contour. For convenience, we have decomposed the self-energies into the first-order

(self-consistent Hartree-Fock) contribution, \mathbf{S}^{HF} (Σ^{HF}) and the higher-order part, \mathbf{S} (Σ), which accounts for inelastic collisions. Collisional self-energies, which are responsible for dissipation and equilibration, can be derived within self-consistent second-order approximation. The bare 2×2 propagator \mathbf{G}_0 is defined as

$$\mathbf{G}_0^{-1}(1, 1') = \delta(1 - 1') \left[i\tau_3 \frac{\partial}{\partial t_1} - \left(-\frac{1}{2m} \Delta_1 + V_{ext}(1) \right) \mathbb{1} \right] \quad (23)$$

where

$$\tau_3 = \begin{pmatrix} 1 & 0 \\ 0 & -1 \end{pmatrix}, \quad (24)$$

and $\mathbb{1}$ is the 2×2 identity matrix in Bogoliubov space. The Hartree-Fock self-energies correspond to the one-particle irreducible diagrammatic contributions of the first order in the interaction strength g

$$\mathbf{S}^{HF}(1, 1') = ig\delta(1 - 1')\mathbf{G}(1, 1') + \frac{i}{2}g\delta(1 - 1') \{ \text{Tr} [\mathbf{C}(1, 1)] + \text{Tr}[\mathbf{G}(1, 1)] \} \mathbb{1}, \quad (25)$$

$$\begin{aligned} \Sigma^{HF}(1, 1') &= ig\delta(1 - 1') \{ \mathbf{G}(1, 1') + \mathbf{C}(1, 1') \} \\ &+ \frac{i}{2}g\delta(1 - 1') \{ \text{Tr} [\mathbf{C}(1, 1)] + \text{Tr}[\mathbf{G}(1, 1)] \} \mathbb{1}. \end{aligned} \quad (26)$$

Parametrizing the Keldysh contour in terms of real time variable we obtain from Eqs. (21) and (22),

$$\int_{-\infty}^{\infty} d2 [\mathbf{G}_0^{-1}(1, 2) - \mathbf{S}^{HF}(1, 2)] \mathbf{C}(2, 1') = -i \int_{-\infty}^{t_1} d2 \gamma(1, 2) \mathbf{C}(2, 1'), \quad (27)$$

$$\begin{aligned} &\int_{-\infty}^{\infty} d2 [\mathbf{G}_0^{-1}(1, 2) - \Sigma^{HF}(1, 2)] \mathbf{G}^{\geq}(2, 1') = \\ &-i \left[\int_{-\infty}^{t_1} d2 \Gamma(1, 2) \mathbf{G}^{\geq}(2, 1') - \int_{-\infty}^{t_{1'}} d2 \Sigma^{\geq}(1, 2) \mathbf{A}(2, 1') \right]. \end{aligned} \quad (28)$$

Here we introduced the QP spectral function

$$\mathbf{A}(1, 1') = i [\mathbf{G}^>(1, 1') - \mathbf{G}^<(1, 1')] \quad (29)$$

and analogously,

$$\Gamma(1, 1') = i [\Sigma^>(1, 1') - \Sigma^<(1, 1')], \quad (30)$$

and

$$\gamma(1, 1') = i [\mathbf{S}^>(1, 1') - \mathbf{S}^<(1, 1')] \quad (31)$$

for the corresponding self-energies not containing the Hartree-Fock contributions. The "lesser" and "greater" Green's functions are defined as usual [42],

$$\mathbf{G}^<(1, 1') = -i \begin{pmatrix} \langle \tilde{\Psi}^\dagger(1') \tilde{\Psi}(1) \rangle & \langle \tilde{\Psi}(1') \tilde{\Psi}(1) \rangle \\ \langle \tilde{\Psi}^\dagger(1') \tilde{\Psi}^\dagger(1) \rangle & \langle \tilde{\Psi}(1') \tilde{\Psi}^\dagger(1) \rangle \end{pmatrix} = \begin{pmatrix} G^<(1, 1') & F^<(1, 1') \\ \overline{F}^<(1, 1') & \overline{G}^<(1, 1') \end{pmatrix}, \quad (32)$$

$$\mathbf{G}^>(1, 1') = -i \begin{pmatrix} \langle \tilde{\Psi}(1) \tilde{\Psi}^\dagger(1') \rangle & \langle \tilde{\Psi}(1) \tilde{\Psi}(1') \rangle \\ \langle \tilde{\Psi}^\dagger(1) \tilde{\Psi}^\dagger(1') \rangle & \langle \tilde{\Psi}^\dagger(1) \tilde{\Psi}(1') \rangle \end{pmatrix} = \begin{pmatrix} G^>(1, 1') & F^>(1, 1') \\ \overline{F}^>(1, 1') & \overline{G}^>(1, 1') \end{pmatrix}. \quad (33)$$

It is, furthermore, convenient to introduce the so-called statistical propagator (which is just the Keldysh component of the QP Green's function $\mathbf{G}^K(1, 1')$ divided by two),

$$\mathbf{F}(1, 1') = \frac{\mathbf{G}^>(1, 1') + \mathbf{G}^<(1, 1')}{2}, \quad (34)$$

and rewrite our equations in terms of the spectral function and the statistical propagator which contain the information about the spectrum and the occupation number, respectively.

We hence get,

$$\int_{-\infty}^{\infty} d2 [\mathbf{G}_0^{-1}(1, 2) - \Sigma^{HF}(1, 2)] \mathbf{A}(2, 1') = -i \int_{t_{1'}}^{t_1} d2 \Gamma(1, 2) \mathbf{A}(2, 1') \quad (35)$$

and

$$\begin{aligned} \int_{-\infty}^{\infty} d2 [\mathbf{G}_0^{-1}(1, 2) - \Sigma^{HF}(1, 2)] \mathbf{F}(2, 1') = \\ - i \left[\int_{-\infty}^{t_1} d2 \Gamma(1, 2) \mathbf{F}(2, 1') - \int_{-\infty}^{t_{1'}} d2 \Pi(1, 2) \mathbf{A}(2, 1') \right], \end{aligned} \quad (36)$$

where Π is defined as,

$$\Pi(1, 1') = \frac{\Sigma^>(1, 1') + \Sigma^<(1, 1')}{2}. \quad (37)$$

Eqs. (35) and (36) were obtained by taking the difference and the sum of Eq. (28) for the "greater" and "lesser" propagator, and then inserting the definition of the spectral function (29) and the statistical function (34), respectively. The Hartree-Fock self-energies in terms of the spectral and statistical functions read

$$\mathbf{S}^{HF}(1, 1') = ig\delta(1 - 1')\mathbf{F}(1, 1') + \frac{i}{2}g\delta(1 - 1') \{ \text{Tr} [\mathbf{C}(1, 1)] + \text{Tr} [\mathbf{F}(1, 1)] \} \mathbb{1}, \quad (38)$$

$$\begin{aligned}\Sigma^{HF}(1, 1') &= ig\delta(1 - 1') \{\mathbf{F}(1, 1') + \mathbf{C}(1, 1')\} \\ &+ \frac{i}{2}g\delta(1 - 1') \{\text{Tr}[\mathbf{C}(1, 1)] + \text{Tr}[\mathbf{F}(1, 1)]\} \mathbf{1},\end{aligned}\tag{39}$$

where we used $\mathbf{G}^<(1, 1')|_{t_1=t_{1'}} = \mathbf{F}(1, 1')|_{t_1=t_{1'}} + i\mathbf{1}\delta(\mathbf{r}_1 - \mathbf{r}'_1)/2$. (The terms proportional to $\delta(\mathbf{r}_1 - \mathbf{r}'_1)$ are not explicitly written in the equations to shorten the notation). It is worth mentioning that these self-energies only contain the symmetrized two-point propagators instead of the time-ordered ones. The non-condensate and the anomalous density are then expressed in terms of the propagators $G^<$ and $F^<$, evaluated at equal points in space and time.

We now derive from our general Dyson equations the equations of motion for the condensates and the QP excitations in the eigenbasis \mathbb{B} of the trap potential.

B. Condensate equation of motion in the trap eigenbasis

Using the bosonic field operator (5), we straightforwardly obtain for the propagators (19) and (20), the spectral function (29) and the statistical function (34) the following expressions,

$$\mathbf{G}(1, 1') = \sum_{n,m=1}^M \varphi_m(\mathbf{r})\varphi_n(\mathbf{r}')\mathbf{G}_{nm}(t, t')\tag{40}$$

$$\mathbf{C}(1, 1') = \sum_{\alpha,\beta=1}^2 \phi_\alpha(\mathbf{r})\phi_\beta(\mathbf{r}')\mathbf{C}_{\alpha\beta}(t, t'),\tag{41}$$

$$\mathbf{A}(1, 1') = \sum_{n,m=1}^M \varphi_m(\mathbf{r})\varphi_n(\mathbf{r}')\mathbf{A}_{nm}(t, t'),\tag{42}$$

$$\mathbf{F}(1, 1') = \sum_{n,m=1}^M \varphi_m(\mathbf{r})\varphi_n(\mathbf{r}')\mathbf{F}_{nm}(t, t'),\tag{43}$$

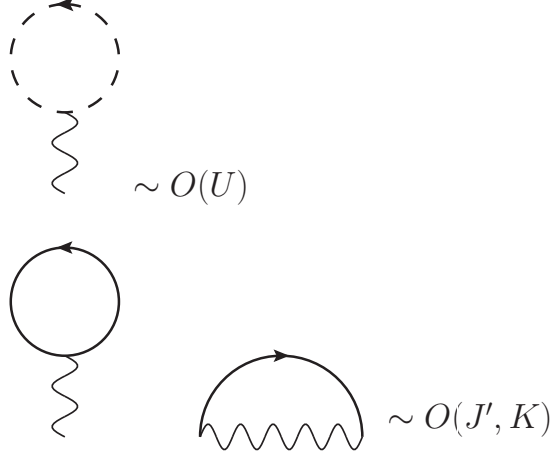


FIG. 2: Hartree-Fock self-energies for the condensate propagator $\mathcal{S}_{\alpha\beta}^{HF}$. The solid and dash lines represent the 2×2 single particle excitations propagator and the condensate propagator, respectively. The wavy lines denote the interactions K, J' or U , depending on which particles are involved in the process. Note that the condensate and the non-condensate propagators in these expressions are non-diagonal in the condensate index α and the QP index m , respectively, since they are the interacting propagators calculated self-consistently from the equations of motion (52), (59), (60).

where

$$\mathbf{G}_{nm}(t, t') = -i \begin{pmatrix} \langle T_C \hat{b}_n(t) \hat{b}_m^\dagger(t') \rangle & \langle T_C \hat{b}_n(t) \hat{b}_m(t') \rangle \\ \langle T_C \hat{b}_n^\dagger(t) \hat{b}_m^\dagger(t') \rangle & \langle T_C \hat{b}_n^\dagger(t) \hat{b}_m(t') \rangle \end{pmatrix} = \begin{pmatrix} G_{nm}(1, 1') & F_{nm}(1, 1') \\ \bar{F}_{nm}(1, 1') & \bar{G}_{nm}(1, 1') \end{pmatrix} \quad (44)$$

$$\mathbf{C}_{\alpha\beta}(t, t') = -i \begin{pmatrix} a_\alpha(t) a_\beta^*(t') & a_\alpha(t) a_\beta(t') \\ a_\alpha^*(t) a_\beta^*(t') & a_\alpha^*(t) a_\beta(t') \end{pmatrix}, \quad (45)$$

$$\mathbf{A}_{nm}(t, t') = \begin{pmatrix} A_{nm}^G(t, t') & A_{nm}^F(t, t') \\ -A_{nm}^F(t, t')^* & -A_{nm}^G(t, t')^* \end{pmatrix}, \quad (46)$$

$$\mathbf{F}_{nm}(t, t') = \begin{pmatrix} F_{nm}^G(t, t') & F_{nm}^F(t, t') \\ -F_{nm}^F(t, t')^* & -F_{nm}^G(t, t')^* \end{pmatrix}, \quad (47)$$

with $A_{nm}^G = i(G_{nm}^> - G_{nm}^<)$, $A_{nm}^F = i(F_{nm}^> - F_{nm}^<)$ and $F_{nm}^G = (G_{nm}^> + G_{nm}^<)/2$, and $F_{nm}^F = (F_{nm}^> + F_{nm}^<)/2$. Here and in the following, Greek indices, $\alpha, \beta = 1, 2$, refer to the condensates in the left and right wells, and latin indices, $n, m = 1, 2, \dots, M$, denote the QP levels. Moreover, we will adopt the sum convention, i.e., Greek or Latin indices appearing in a term twice are summed over.

Inserting Eqs. (41), (42) and (43) into the Dyson equation for the condensate Green's function, (27) we obtain the Dyson equation for $\mathbf{C}_{\alpha\beta}(t, t')$, where the position dependence is absorbed in the parameters E_0, U, U', K, J and J' ,

$$\int_{-\infty}^{\infty} d\bar{t} [\mathbf{G}_{0,\alpha\gamma}^{-1}(t, \bar{t}) - \mathbf{S}_{\alpha\gamma}^{HF}(t, \bar{t})] \mathbf{C}_{\gamma\beta}(\bar{t}, t') = -i \int_{-\infty}^t d\bar{t} \gamma_{\alpha\gamma}(t, \bar{t}) \mathbf{C}_{\gamma\beta}(\bar{t}, t'). \quad (48)$$

In this equation, $\gamma_{\alpha\beta} = \mathbf{S}_{\alpha\beta}^> - \mathbf{S}_{\alpha\beta}^<$ accounts for collisions. The bare propagator is given by

$$\mathbf{G}_{0,\alpha\beta}^{-1}(t, t') = \left[i\tau_3 \delta_{\alpha\beta} \frac{\partial}{\partial t} - \mathbf{1} E_{\alpha\beta} \right] \delta(t - t'), \quad (49)$$

with $E_{11} = E_{22} = E_0$ and $E_{12} = E_{21} = -J$. The Hartree-Fock self-energies read,

$$\begin{aligned} \mathbf{S}_{\alpha\alpha}^{HF}(t, t') &= \frac{i}{2} U \text{Tr} [\mathbf{C}_{\alpha\alpha}(t, t)] \mathbf{1} \delta(t - t') + \\ &+ i \frac{K}{2} \sum_{n,m=1}^M \left\{ \frac{1}{2} \text{Tr} [\mathbf{F}_{nm}^<(t, t)] \mathbf{1} + \mathbf{F}_{nm}^<(t, t) \right\} \delta(t - t') \end{aligned} \quad (50)$$

$$\begin{aligned} \mathbf{S}_{12}^{HF}(t, t') &= \mathbf{S}_{21}^{HF}(t, t') = \\ &+ i \frac{J'}{2} \sum_{n,m=1}^M \left\{ \frac{1}{2} \text{Tr} [\mathbf{F}_{nm}^<(t, t)] \mathbf{1} + \mathbf{F}_{nm}^<(t, t) \right\} \delta(t - t'), \end{aligned} \quad (51)$$

In Fig. 2 the diagrammatic representation of the self-energy (51) is given. After evaluating the integral on the left-hand side of Eq. (48), the equation of motion for the condensate propagator reads,

$$\left[i\tau_3 \delta_{\alpha\gamma} \frac{\partial}{\partial t} - \mathbf{1} E_{\alpha\gamma} - \mathbf{S}_{\alpha\gamma}^{HF}(t) \right] \mathbf{C}_{\gamma\beta}(t, t') = -i \int_{-\infty}^t d\bar{t} \gamma_{\alpha\gamma}(t, \bar{t}) \mathbf{C}_{\gamma\beta}(\bar{t}, t'), \quad (52)$$

where we used that $\mathbf{S}_{\alpha\gamma}^{HF}(t, t') = \mathbf{S}_{\alpha\gamma}^{HF}(t) \delta(t - t')$. The equation of motion for the time-dependent condensate amplitude $a_\alpha(t)$ can be obtained by taking the upper left component of Eq. (52) and then dividing by $a_\beta^*(t')$,

$$i \frac{\partial}{\partial t} a_\alpha = [E_{\alpha\gamma} + S_{\alpha\gamma}^{HF}(t)] a_\gamma(t) + W_{\alpha\gamma}^{HF}(t) a_\gamma^*(t) - i \int_{-\infty}^t d\bar{t} [\gamma_{\alpha\gamma}^S(t, \bar{t}) a_\gamma(\bar{t}) + \gamma_{\alpha\gamma}^W(t, \bar{t}) a_\gamma(\bar{t}) a_\gamma^*(\bar{t})], \quad (53)$$

where $S_{\alpha\beta}^{HF}$ and $W_{\alpha\beta}^{HF}$ are the upper left and the upper right components of $\mathbf{S}_{\alpha\beta}^{HF}$, defined in Eq. (51), i.e.,

$$\mathbf{S}_{\alpha\beta}^{HF}(t) = \begin{pmatrix} S_{\alpha\beta}^{HF}(t) & W_{\alpha\beta}^{HF}(t) \\ W_{\alpha\beta}^{HF}(t)^* & S_{\alpha\beta}^{HF}(t)^* \end{pmatrix}. \quad (54)$$

Similarly, $\gamma_{\alpha\beta}^S$ and $\gamma_{\alpha\beta}^W$ are the upper left and the upper right components of $\gamma_{\alpha\beta}$, respectively.

C. Quasiparticle equations of motion in the trap eigenbasis

We follow here the procedure analogous to the one described in the previous section for the evolution Eqs. (35) and (36) for non-condensate particle spectral and statistical functions. Inserting Eqs. (42) and (43) into Eqs. (35) and (36) we get,

$$\int_{-\infty}^{\infty} d\bar{t} [\mathbf{G}_{0,n\ell}^{-1}(t, \bar{t}) - \Sigma_{n\ell}^{HF}(t, \bar{t})] \mathbf{A}_{\ell m}(\bar{t}, t') = -i \int_{t'}^t d\bar{t} \mathbf{\Gamma}_{n\ell}(t, \bar{t}) \mathbf{A}_{\ell m}(\bar{t}, t') \quad (55)$$

$$\begin{aligned} \int_{-\infty}^{\infty} d\bar{t} [\mathbf{G}_{0,n\ell}^{-1}(t, \bar{t}) - \Sigma_{n\ell}^{HF}(t, \bar{t})] \mathbf{F}_{\ell m}(\bar{t}, t') = & -i \left[\int_{-\infty}^t d\bar{t} \mathbf{\Gamma}_{n\ell}(t, \bar{t}) \mathbf{F}_{\ell m}(\bar{t}, t') \right. \\ & \left. - \int_{-\infty}^{t'} d\bar{t} \mathbf{\Pi}_{n\ell}(t, \bar{t}) \mathbf{A}_{\ell m}(\bar{t}, t') \right], \end{aligned} \quad (56)$$

where $\mathbf{\Pi}_{nm} = (\Sigma_{nm}^> + \Sigma_{nm}^<)/2$ and $\mathbf{\Gamma}_{nm} = \Sigma_{nm}^> - \Sigma_{nm}^<$. The bare one-particle propagator and the Hartree-Fock self-energy are given by

$$\mathbf{G}_{0,nm}^{-1}(t, t') = \left[i\tau_3 \frac{\partial}{\partial t} - \epsilon_n \mathbb{1} \right] \delta_{nm} \delta(t - t'), \quad (57)$$

$$\begin{aligned} \Sigma_{nm}^{HF}(t, t') = & i \left(\sum_{\alpha, \beta=1}^2 K_{\alpha\beta nm} \left\{ \mathbf{C}_{\alpha\beta}(t, t) + \frac{1}{2} \text{Tr} [\mathbf{C}_{\alpha\beta}(t, t)] \mathbb{1} \right\} \right. \\ & \left. + U' \sum_{\ell, s \neq 0} \left\{ \mathbf{F}_{\ell s}(t, t) + \frac{1}{2} \text{Tr} [\mathbf{F}_{\ell s}(t, t)] \mathbb{1} \right\} \right) \delta(t - t'), \end{aligned} \quad (58)$$

where ϵ_n , U' and $K_{\alpha\beta nm}$ are defined in Eqs. (12), (13) and (15). The first-order contributions to the self-energy of QP excitations in Eq. (58) are shown in Fig. 3. Evaluation of the integrals on the left-hand side of Eqs. (55) and (56) yields,

$$\left[i\tau_3 \delta_{n\ell} \frac{\partial}{\partial t} - \epsilon_n \delta_{n\ell} \mathbb{1} - \Sigma_{n\ell}^{HF}(t) \right] \mathbf{A}_{\ell m}(t, t') = -i \int_{t'}^t d\bar{t} \mathbf{\Gamma}_{n\ell}(t, \bar{t}) \mathbf{A}_{\ell m}(\bar{t}, t'), \quad (59)$$

$$\begin{aligned} \left[i\tau_3 \delta_{n\ell} \frac{\partial}{\partial t} - \epsilon_n \delta_{n\ell} \mathbb{1} - \Sigma_{n\ell}^{HF}(t) \right] \mathbf{F}_{\ell m}(t, t') = & -i \left[\int_{-\infty}^t d\bar{t} \mathbf{\Gamma}_{n\ell}(t, \bar{t}) \mathbf{F}_{\ell m}(\bar{t}, t') \right. \\ & \left. - \int_{-\infty}^{t'} d\bar{t} \mathbf{\Pi}_{n\ell}(t, \bar{t}) \mathbf{A}_{\ell m}(\bar{t}, t') \right], \end{aligned} \quad (60)$$

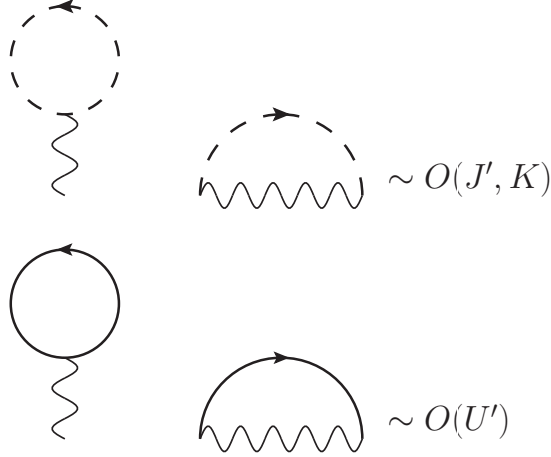


FIG. 3: Diagrammatic contributions to the Hartree-Fock self-energies of non-condensed particles Σ_{nm}^{HF} . The solid and dashed lines represent the 2×2 single-particle excitation propagator and the condensate propagator, respectively. The wavy lines denote the interactions K, J' or U' , depending on which physical process of the Hamiltonian is involved.

where we used that $\Sigma_{nm}^{HF}(t, t') = \Sigma_{nm}^{HF}(t)\delta(t - t')$.

Computing the evolution of \mathbf{F}_{nm} for equal time arguments requires special attention. In order to do it properly, we take the sum and the difference of Eq. (60) and its hermitean conjugate, and evaluate it at equal times (see details in the next section). Note, that the components of $\mathbf{A}_{nm}(t, t)$ are fixed for all times due to the bosonic commutation relations. One must also obey particle and energy conservation by applying conserving approximations - for details see the Appendix.

Eqs. (52), (59) and (60) constitute the general equations of motion for the condensate and the non-condensate (spectral and statistical) propagators, respectively. They are coupled via the self-energies which are functions of these propagators and must be evaluated self-consistently in order to obtain a conserving approximation (see Appendix). The time-dependent Hartree-Fock self-energies describe the dynamical shift of the condensate and the single-particle levels due to the dynamical change of their occupation numbers and their interactions. The higher order interaction terms on the right-hand side of the equations of motion describe inelastic QP collisions. They are, in general, responsible for QP damping, damping of the condensate oscillations and for thermalization. In the present paper, we are interested in how the non-equilibrium condensate oscillations induce QP excitations and

how the latter act back on the condensate dynamics. Hence, we do not consider QP collision effects here. The results including collisions will be published elsewhere [40].

IV. EQUATIONS OF MOTION IN BOGOLIUBOV-HARTREE-FOCK APPROXIMATION

We now neglect collisional terms and treat the non-equilibrium Bose Josephson junction within Bogoliubov-Hartree-Fock approximation. From Eqs. (53) and (60) we get,

$$i\frac{\partial}{\partial t}a_\alpha = [E_{\alpha\gamma} + S_{\alpha\gamma}^{HF}(t)] a_\gamma(t) + W_{\alpha\gamma}^{HF}(t)a_\gamma^*(t), \quad (61)$$

$$i\tau_3\delta_{n\ell}\frac{\partial}{\partial t}\mathbf{F}_{\ell m}(t, t') = [\epsilon_n\delta_{n\ell}\mathbf{1} + \Sigma_{n\ell}^{HF}(t)] \mathbf{F}_{\ell m}(t, t'). \quad (62)$$

It is not necessary to consider the equations for the spectral function \mathbf{A}_{nm} , since the only non-condensate related quantities appearing in the self-energies $\mathbf{S}_{\alpha\beta}^{HF}$ and Σ_{nm}^{HF} are the components of the statistical function \mathbf{F}_{nm} . This implies that Eqs. (61) and (62) decouple completely from the equations for \mathbf{A}_{nm} . This will not be the case when collisions are taken into account. Taking the difference of Eq. (62) and its hermitean conjugate, we get for its diagonal component,

$$i\left(\frac{\partial}{\partial t}F_{nm}^G(t, t') + \frac{\partial}{\partial t'}F_{nm}^G(t, t')\right) = [\epsilon_n\delta_{n\ell} + \Sigma_{n\ell}^{HF}(t)] F_{\ell m}^G(t, t') - \Omega_{n\ell}^{HF}(t)F_{\ell m}^F(t, t')^* - F_{n\ell}^G(t, t') [\epsilon_m\delta_{m\ell} + \Sigma_{\ell m}^{HF}(t')] - F_{n\ell}^F(t, t')\Omega_{\ell m}^{HF}(t')^* \quad (63)$$

The sum of Eq. (62) and its hermitean conjugate gives for its upper right component,

$$i\left(\frac{\partial}{\partial t}F_{nm}^F(t, t') + \frac{\partial}{\partial t'}F_{nm}^F(t, t')\right) = [\epsilon_n\delta_{n\ell} + \Sigma_{n\ell}^{HF}(t)] F_{\ell m}^F(t, t') - \Omega_{n\ell}^{HF}(t)F_{\ell m}^G(t, t')^* + F_{n\ell}^F(t, t') [\epsilon_m\delta_{m\ell} + \Sigma_{\ell m}^{HF}(t')] + F_{n\ell}^G(t, t')\Omega_{\ell m}^{HF}(t')^* \quad (64)$$

Here we adopted the notation,

$$\Sigma_{nm}^{HF}(t) = \begin{pmatrix} \Sigma_{nm}^{HF}(t) & \Omega_{nm}^{HF}(t) \\ \Omega_{nm}^{HF}(t)^* & \Sigma_{nm}^{HF}(t)^* \end{pmatrix}. \quad (65)$$

The self-energies $\Sigma_{nm}^{HF}(t)$ and $\Omega_{nm}^{HF}(t)$ are given by,

$$\Sigma_{nm}^{HF}(t) = K(N_1(t) + N_2(t)) + J'a_1^*(t)a_2(t) + J'a_2^*(t)a_1(t) + 2iU' \sum_{s,\ell} F_{s\ell}^G(t, t), \quad (66)$$

$$\Omega_{nm}^{HF}(t) = \frac{K}{2} \sum_{\alpha=1}^2 a_\alpha(t)a_\alpha(t) + J'a_1(t)a_2(t) + iU' \sum_{s,\ell} F_{s\ell}^F(t, t), \quad (67)$$

where $N_\alpha = a_\alpha^* a_\alpha$, $\alpha = 1, 2$. Evaluation of eq. (63) and (64) at equal times gives,

$$i \frac{\partial}{\partial t} F_{nm}^G(t, t) = [\epsilon_n \delta_{n\ell} + \Sigma_{n\ell}^{HF}(t)] F_{\ell m}^G(t, t) - F_{n\ell}^G(t, t) [\epsilon_m \delta_{m\ell} + \Sigma_{\ell m}^{HF}(t)] \\ - \Omega_{n\ell}^{HF}(t) F_{\ell m}^F(t, t)^* - F_{n\ell}^F(t, t) \Omega_{\ell m}^{HF}(t)^*, \quad (68)$$

$$i \frac{\partial}{\partial t} F_{nm}^F(t, t) = [\epsilon_n \delta_{n\ell} + \Sigma_{n\ell}^{HF}(t)] F_{\ell m}^F(t, t) + F_{n\ell}^F(t, t) [\epsilon_m \delta_{m\ell} + \Sigma_{\ell m}^{HF}(t)] \\ - \Omega_{n\ell}^{HF}(t) F_{\ell m}^G(t, t)^* + F_{n\ell}^G(t, t) \Omega_{\ell m}^{HF}(t)^*. \quad (69)$$

Note, that in our previous work [21] we considered a special case of the functions F_{nm}^G and F_{nm}^F (or their equivalents) being diagonal in energy space, i.e. being proportional to δ_{nm} . In this work we do not adhere to this approximation and solve Eqs. (68) and (69) for all n and m . Plugging the expressions for $S_{\alpha\beta}^{HF}$ and $W_{\alpha\beta}^{HF}$ into Eq. (61) we obtain,

$$i \frac{\partial}{\partial t} a_1(t) = \left[E_0 + U N_1(t) + iK \sum_{n,m} F_{nm}^G(t, t) \right] a_1(t) - \left[J - iJ' \sum_{n,m} F_{nm}^G(t, t) \right] a_2(t) \\ + i \left[\frac{K}{2} a_1^*(t) + \frac{J'}{2} a_2^*(t) \right] \sum_{n,m} F_{nm}^F(t, t). \quad (70)$$

The equation for $a_2(t)$ is obtained from Eq.(70) by replacing a_1 by a_2 and vice versa.

V. RESULTS

We now solve the system of Eqs. (66) -(70) numerically. We take the initial conditions

$$a_\alpha(0) = \sqrt{N_\alpha(0)} e^{i\theta_\alpha(0)}, \quad (71)$$

$$F_{nm}^G(0, 0) = -\frac{i}{2} \delta_{nm}, \quad (72)$$

$$F_{nm}^F(0, 0) = 0, \quad (73)$$

with $z(0) = 0.6$ and initial phase difference $\theta_1(0) - \theta_2(0) = 0$. The total particle number is taken equal to $N = N_1(0) + N_2(0) = 500000$, with initially all particles in the condensate. It is convenient to define the dimensionless parameters [21] $u = NU/J$, $k = NK/J$, $j' = NJ'/J$, $u' = NU'/J$, and $n_b^{(n)}(t) = N_b^{(n)}(t)/N$ as the relative occupation number of QP level n . For an initially delocalized junction we assume $u = u' = 5$ and for an initially self-trapped junction we take $u = u' = 25$. We then analyze the behaviour of our system depending on k , j' and Δ . In the following, all energies are expressed in units of J , and the time is given in units of $1/J$.

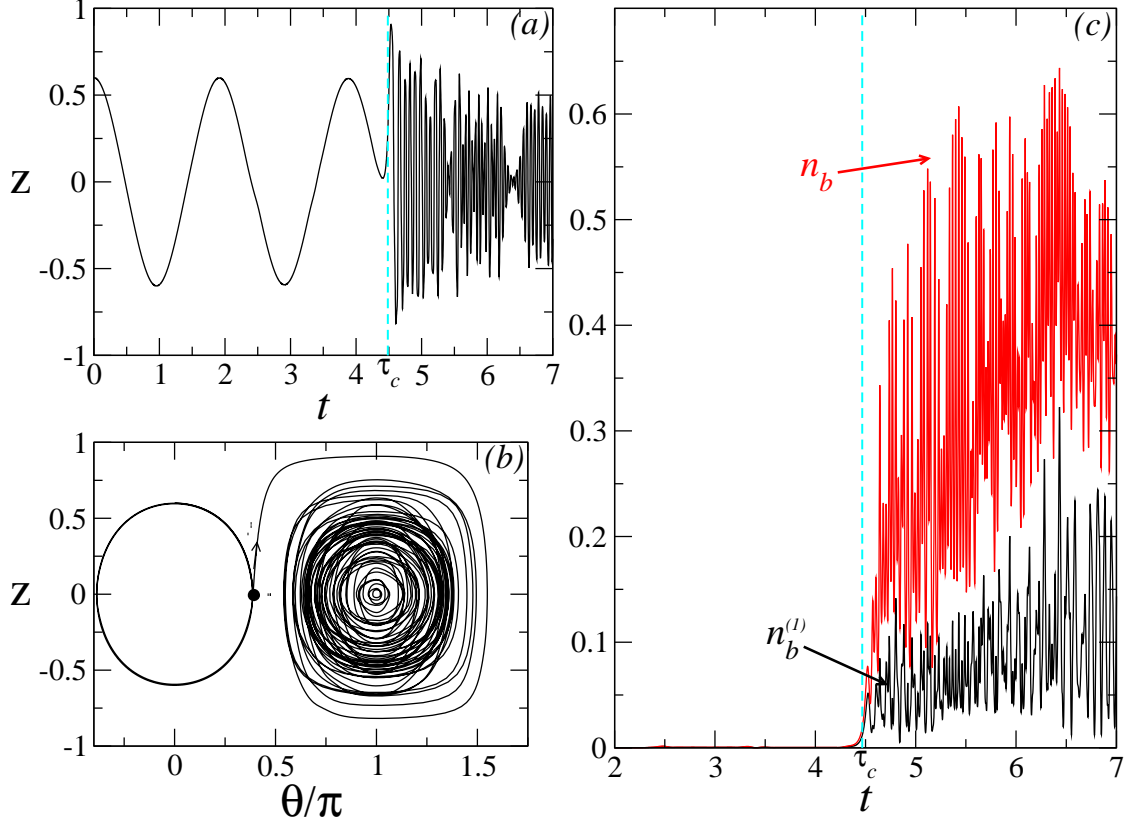


FIG. 4: (a) Time dependence of the particle imbalance z for $z(0) = 0.6, \theta(0) = 0, N = 500000, \Delta = 20.6, u = u' = 5, j' = 60$. (b) Phase portrait of the junction. The thick point on the trajectory corresponds to τ_c , i.e. to an establishing of non-equilibrium dynamics. The arrow shows direction $t > \tau_c$. (c) Time-dependence of the occupation by single-particle excited states of the first level $n_b^{(1)}$, the red curve is the sum of all five levels n_b . The time is given in units of $1/J$.

In the absence of coupling to the single-particle excitations ($J' = K = 0$) or as long as the QP states are not occupied, the equations of motion (52), (59), (60) reduce to Eq. (70) and, hence, for a BEC in a double-well potential, to the well-known two-mode approximation for the BEC dynamics [23], exhibiting undamped Josephson oscillations [21]. Our main result is, however, the appearance of a new characteristic time scale τ_c , which marks the onset of non-equilibrium QP dynamics. It may be surprising at first sight that for a discrete level spectrum τ_c can take a non-zero value [21], i.e., QPs are not excited immediately, even though the initial state with population imbalance $z(0) > 0$ is a highly excited state of the system whose energy exceeds by far the excitation energy of a QP. This is because the BEC

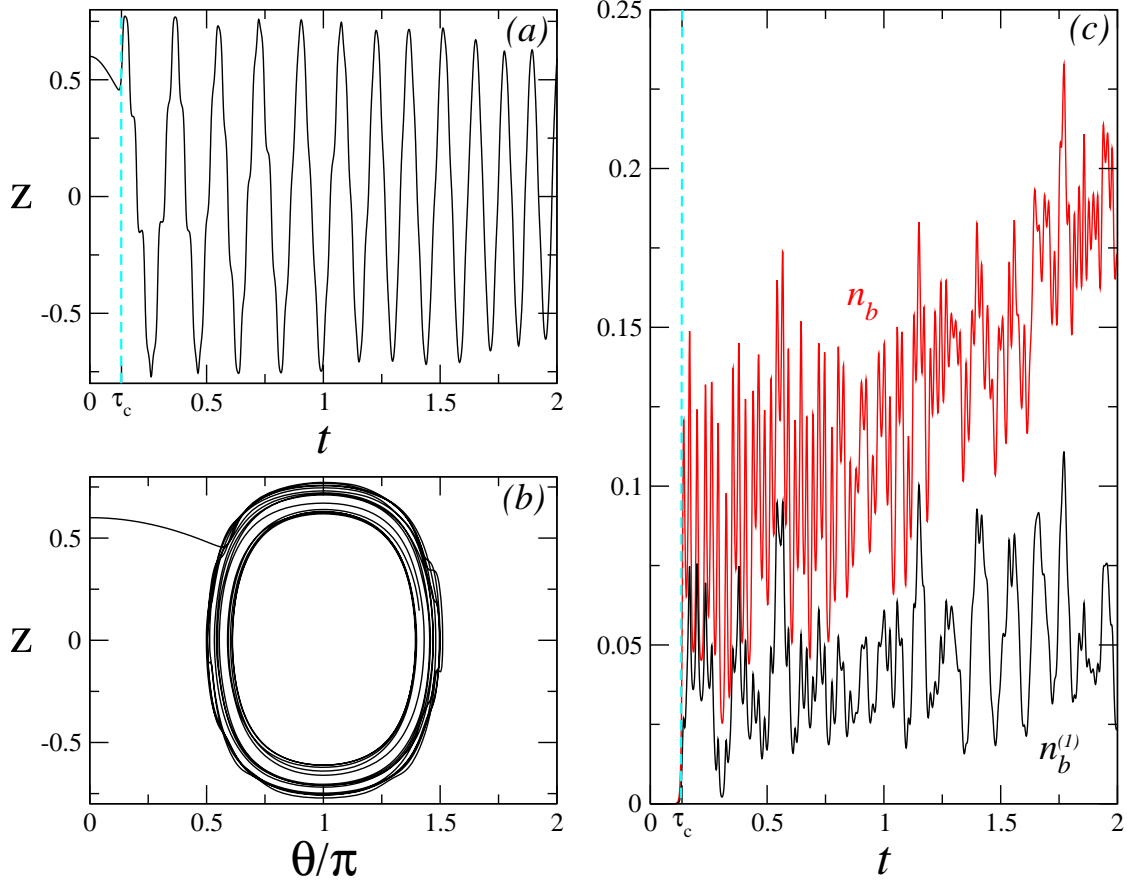


FIG. 5: (a) Time dependence of the particle imbalance z for $z(0) = 0.6, \theta(0) = 0, N = 500000, \Delta = 25, u = u' = 25, j' = 60$. (b) Phase portrait of the junction. (c) Time-dependence of the occupation by single-particle excited states of the first level $n_b^{(1)}$, the red curve is the sum of all five levels n_b . The time is given in units of $1/J$.

Josephson oscillations with frequency $\omega_J \approx 2J\sqrt{1 + u/2}$ [23] act as a periodic perturbation on the QP system, but QPs cannot be excited in low-order time-dependent perturbation theory, if the Josephson frequency is less than the (interaction-renormalized) level spacing, $\omega_J < \Delta_{eff}$ [21]. τ_c depends on system parameters, in particular, the energy splitting Δ and the QP-assisted Josephson coupling j' . We now analyze in detail this new physics.

In Fig. 4(a) the particle imbalance of the initially delocalized junction is shown. One can clearly distinguish two regimes of slow and fast oscillations, respectively. Comparing with Fig. 4(c) reveals that the onset of fast oscillations is marked by an abrupt, avalanche-like population of the single-particle excited states, i.e., it coincides with τ_c . For times $t < \tau_c$ there is only a small, virtual QP population. In this regime, our formalism reduces to the

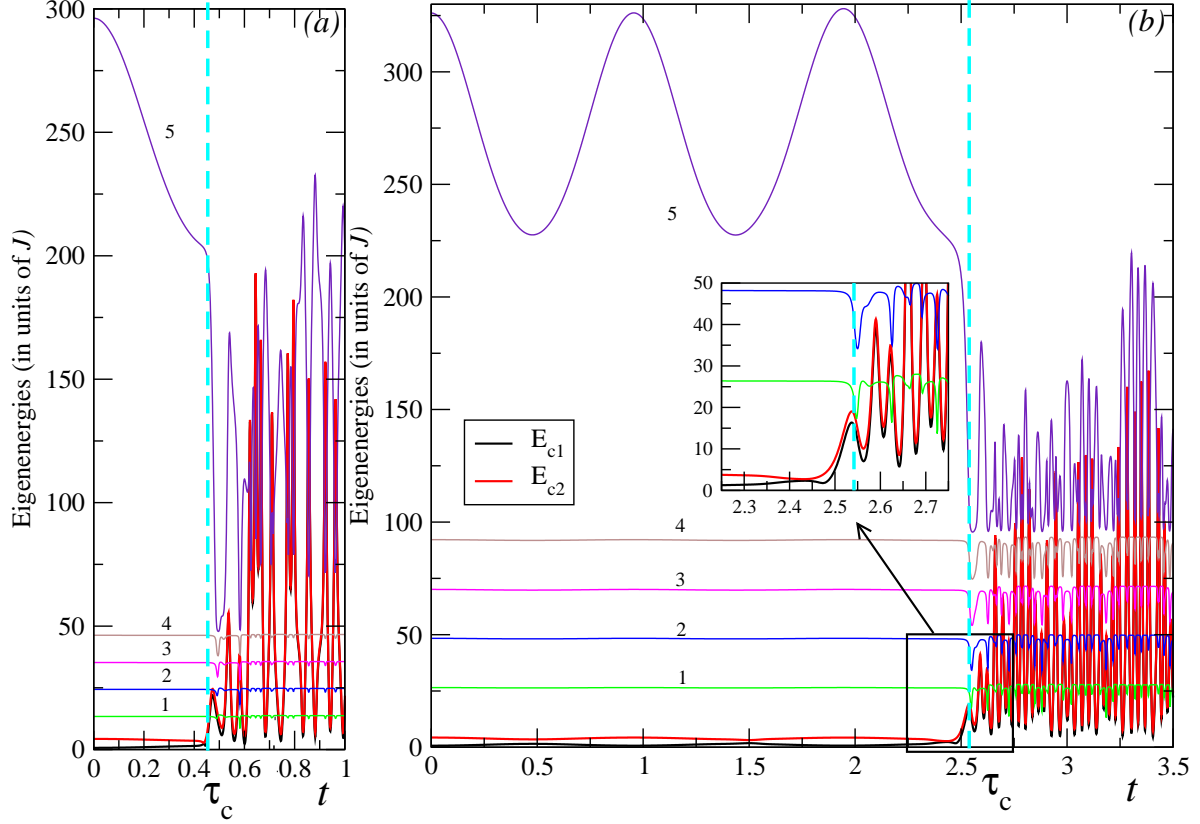


FIG. 6: Instantaneous eigenenergies of the many-body Hamiltonian (6) and extraction of τ_c . Both plots are for $z(0) = 0.6, \theta(0) = 0$, total number of particles is $N = 500000$, $u = u' = 5$, $j' = 60$ and bare level spacing (a) $\Delta = 10$ and (b) $\Delta = 20$. The time is in units of $1/J$. Curves 1 to 5 correspond to the QP eigenenergies E_1, \dots, E_5 . The two lowest curves in the plots correspond to eigenenergies of the condensate in the double well E_{c1} and E_{c2} . A thick vertical line marks the characteristic time τ_c .

two-mode approximation [23] for the condensates, and the dynamics resembles Josephson oscillations. One may, therefore, conjecture that the fast oscillation regime for $t > \tau_c$ is dominated by Rabi oscillations of the single-particle occupation numbers. This will be confirmed below by identifying the oscillation frequencies as the Rabi frequencies for $t > \tau_c$. The drastic change is also seen in the phase portrait of the junction in Fig. 4(b), where the point on the phase trajectory corresponding to τ_c is marked by a thick dot. Before τ_c the time average of the phase difference is equal to zero, as expected in the semiclassical case. However, after τ_c the time average of the phase difference is equal to π . We refer to this kind of behaviour as to "0- π " transition. It may be understood heuristically as follows. One can

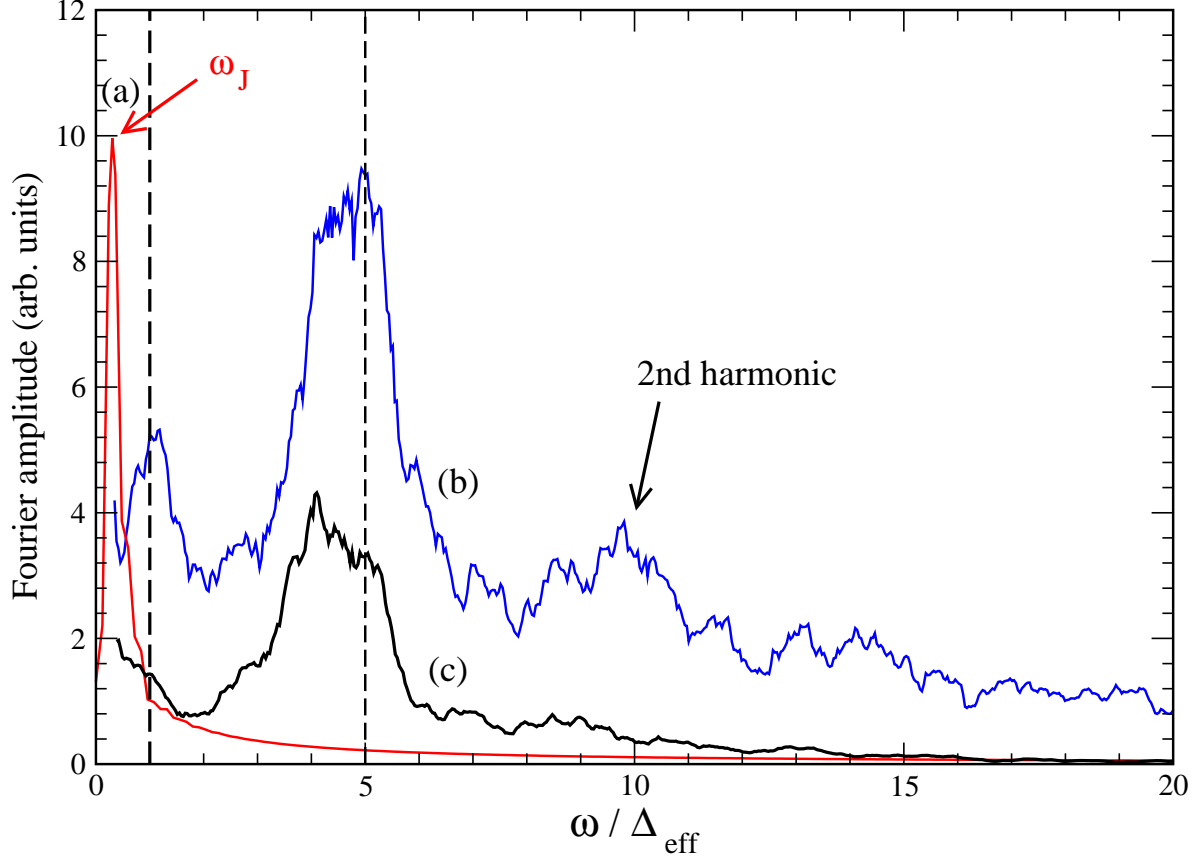


FIG. 7: Fourier transforms of the time traces of Fig. 6 (b) for (a) red curve: first QP level $n = 1$ for $t < \tau_c$, (b) blue curve: first QP level $n = 1$ for $t > \tau_c$ and (c) black curve: condensate mode $\alpha = 1$ for $t > \tau_c$. The renormalized level spacing Δ_{eff} and the spacing between the condensate and the uppermost QP level, $5\Delta_{eff}$, are marked by vertical dashed lines.

think of the two-mode BEC system as a driven oscillator, where the QP system provides the driving force. For $t < \tau_c$ this "oscillator" has no driving force and oscillates at its resonance frequency, i.e., the Josephson frequency ω_J [21, 23], with a phase shift $\theta = 0$. However, once in the regime for $t > \tau_c$, the oscillator is periodically driven at the Rabi frequency, far above its resonance frequency, resulting in a phase shift of $\theta = \pi$.

We observe similar behaviour for the initially self-trapped Bose Josephson junction, shown in Fig. 5. The scale τ_c is substantially smaller in this case (smaller than the period of self-trapped semiclassical oscillations of particle imbalance $T_{ST} \approx 0.6$). At τ_c the junction becomes delocalized and switches to a fast oscillatory regime with the time-averaged phase difference equal to π . The QP occupation numbers show behaviour analogous to that

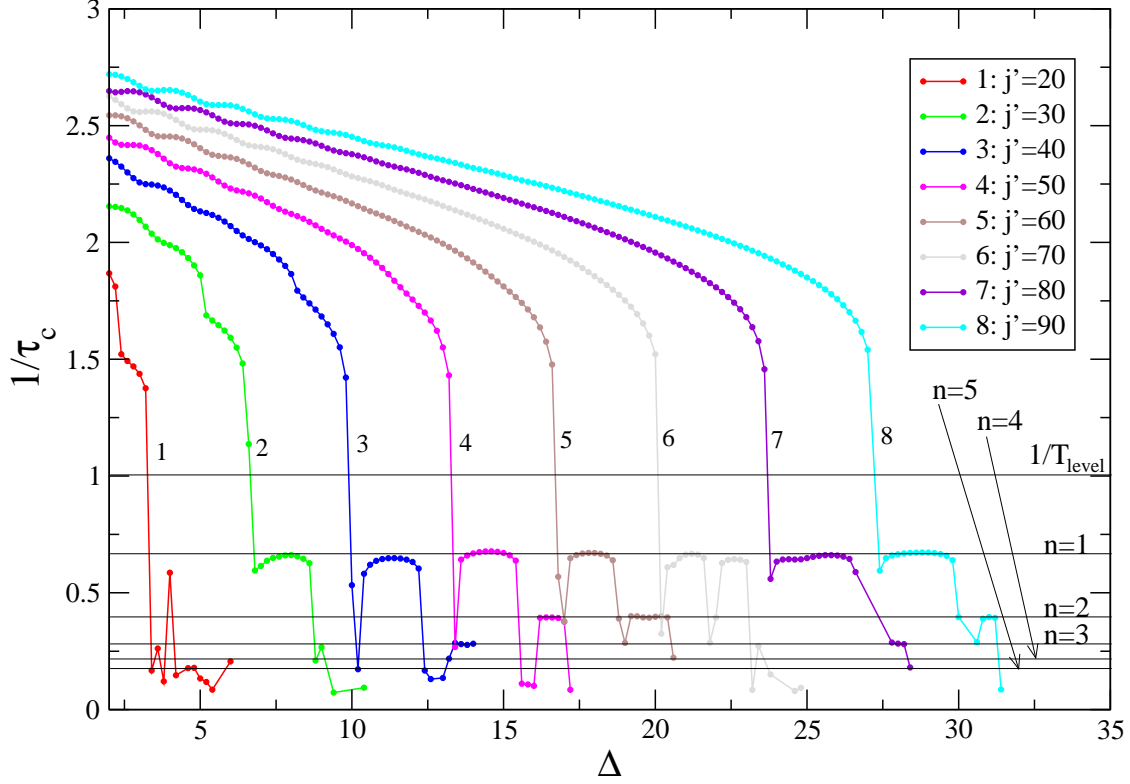


FIG. 8: Dependence of the inverse QP excitation time τ_c^{-1} on the interlevel spacing Δ for an initially delocalized Bose Josephson junction ($n(0) = 0.6$, $\theta(0) = 0$, total number of particles: $N = 500000$, $u = u' = 5$). Different curves are for different values of the QP-assisted Josephson coupling j' . The small dots mark the numerically calculated values. The thin horizontal lines depict the discrete values of the inverse level crossing times, $t_n^{-1} = 2/(2n + 1) T_{level}^{-1}$ for $n = 1, 2, 3, 4, 5$ (see text).

of Fig. 4.

To understand the physical origin of the abrupt onset of the QP-dominated regime and the underlying physics of the fast oscillations for $t \geq \tau_c$, we calculate the instantaneous eigenenergies of the system by diagonalizing the Hamiltonian, including the Bogoliubov-Hartree-Fock renormalizations. These eigenenergies are displayed in Fig. 6 for an initially delocalized junction. Figs. 6(a) and (b) differ only in the value of the bare interlevel spacing Δ . It is seen [inset of Fig. 6 (b)] that τ_c occurs at the moment in time when the highest condensate level E_{c2} (shown in red) crosses the first (renormalized) QP level E_1 for the first time. At this time, QP excitations are no longer blocked energetically, and further QPs are

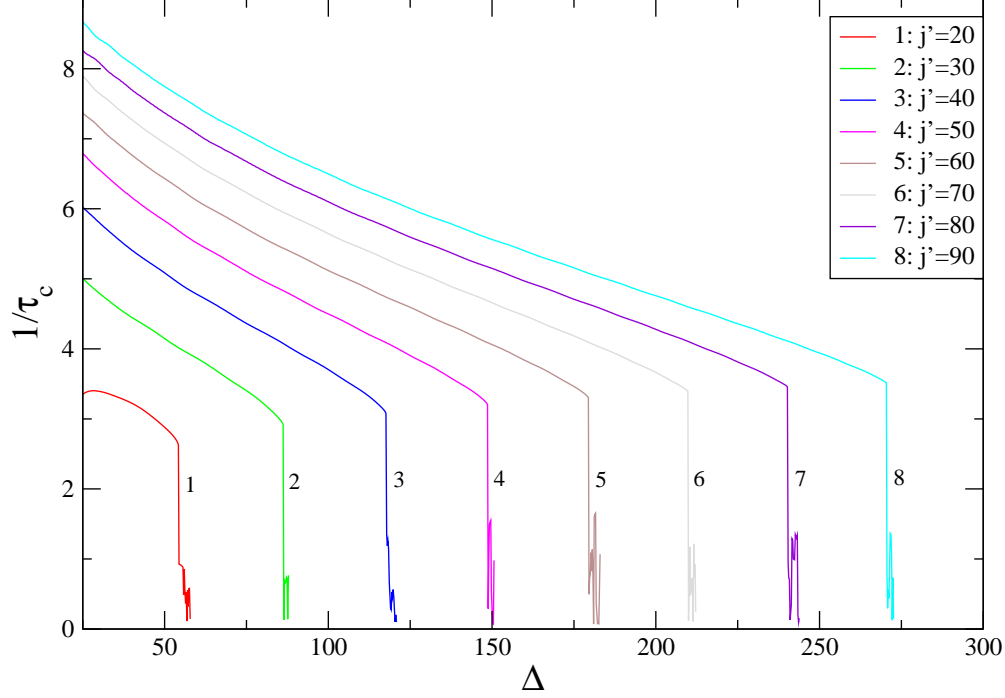


FIG. 9: Dependence of the inverse delocalisation time τ_c^{-1} on the interlevel spacing Δ for an initially self-trapped Bose Josephson junction ($n(0) = 0.6, \theta(0) = 0$, total number of particles is $N = 500000$, $u = u' = 25$). Different curves are for different values of the QP-assisted Josephson coupling j' . The small dots mark the numerically calculated values.

excited resonantly by the fast Rabi oscillations, resulting in an avalanche-like growth of the QP population. We emphasize that this is a highly non-perturbative effect. The time scale τ_c increases as the interlevel spacing grows, compare Figs. 6 (a) and (b). Eventually, it will become impossible to excite QPs, and τ_c will tend to infinity. We note in passing that the uppermost (5th) QP level is pushed upward by a level repulsion effect for $t < \tau_c$, but is pulled down by interactions once it gets populated.

The afore-mentioned fast oscillations can now be identified as Rabi oscillations by comparing their frequency with the renormalized level spacing Δ_{eff} . To that end we plot in Fig. 7 the Fourier transforms of the time traces of the first QP level $E_1(t)$ for $t < \tau_c$ and $t > \tau_c$, respectively, and also the Fourier transform of the BEC level $E_{c1}(t)$ for $t > \tau_c$. Similar results are obtained for the other levels. It is seen that in the QP-dominated regime, $t > \tau_c$, both the condensate and the QP levels oscillate predominantly with frequencies given by the renormalized level spacing, Δ_{eff} , and with the energy spacing between condensate

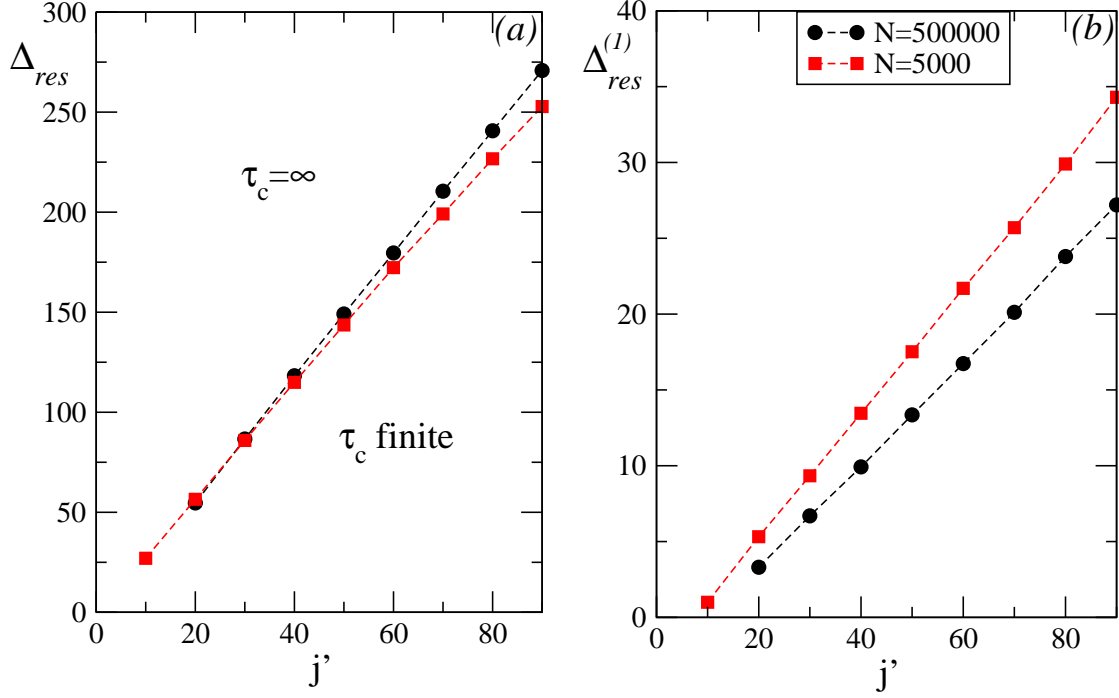


FIG. 10: The interlevel spacing Δ_{res} at which τ_c first takes a discrete value is plotted versus j' for (a) an initially self-trapped junction ($n(0) = 0.6$, $\theta(0) = 0$, $u = u' = 25$) and (b) an initially delocalized junction ($n(0) = 0.6$, $\theta(0) = 0$, $u = u' = 5$), each for two values of the particle number N .

and the uppermost level, $5\Delta_{eff}$. Note that the uppermost level has a large oscillation amplitude, because its oscillation amplitude is not bounded from above by other levels. This unambiguously shows that the fast oscillations are Rabi oscillations.

We now study the detailed dependence of the characteristic time scale τ_c on the level spacing Δ , the QP-assisted tunneling amplitude j' and the condensate-QP scattering amplitude k . The dependence of the inverse τ_c on the interlevel spacing Δ and QP-assisted Josephson coupling j' for the initially delocalized junction is shown in Fig. 8. First, we note that, before QPs get excited, the oscillation period T_{level} of the condensate levels $E_{c1,c2}$, and of the QP levels, E_n , is half the Josephson oscillation period, $T_{level} = 1/2T_J = \pi/\omega_J$, as can be seen from Figs. 4 and 6. This is because the $E_{c1,c2}$, E_n depend on the absolute value $|z(t)|$. In Fig. 8 one can distinguish two regimes of qualitatively different behavior of $1/\tau_c$: For $1/\tau_c > 1/T_{level}$, τ_c depends on Δ in a continuous way, while for $1/\tau_c < 1/T_{level}$ it jumps between certain discrete or plateau values. This is explained as follows. If Δ is small enough

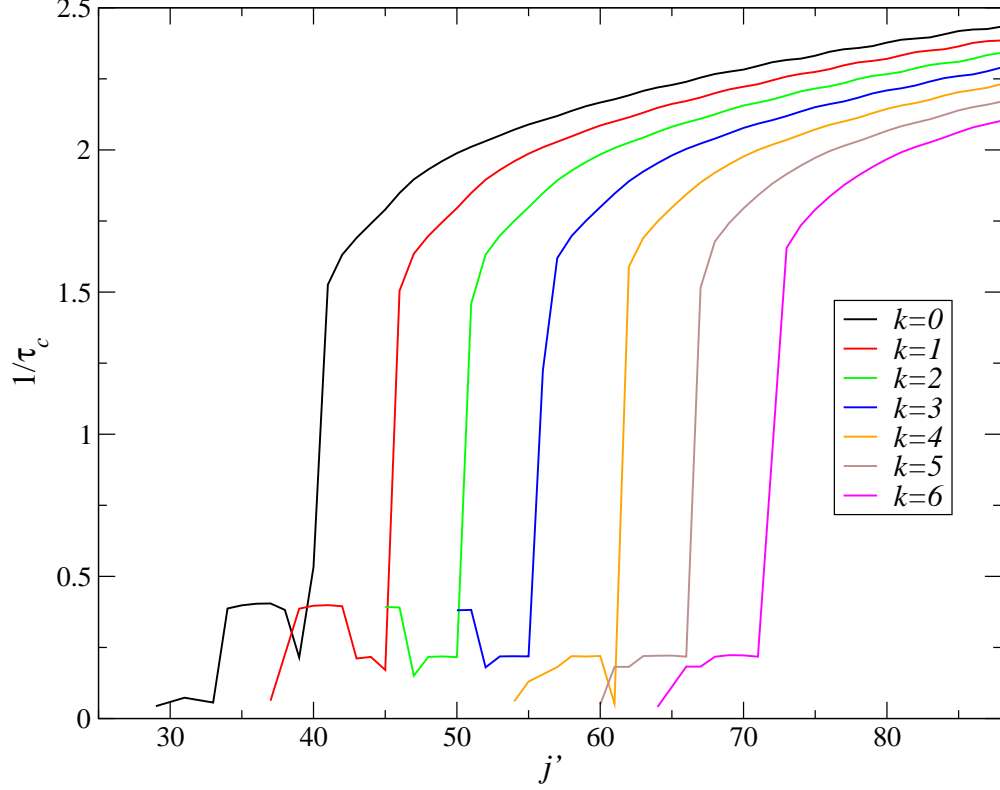


FIG. 11: Dependence of τ_c^{-1} on j' for different values of k and a fixed Δ ($\Delta = 10$). Initially the junction is delocalized: $n(0) = 0.6, \theta(0) = 0, u = u' = 5$; total number of particles: $N = 500000$.

so that $1/\tau_c > 1/T_{level}$, the condensates cannot perform a full Josephson oscillation before QPs get excited. Therefore, the BEC dynamics cannot be considered a periodic perturbation on the QP system, and any value of τ_c is possible, thus increasing continuously with Δ . For $1/\tau_c < 1/T_{level}$, however, the QP system gets excited when one of the BEC levels $E_{c1,c2}$ and the first QP level E_1 come close to each other and eventually cross, see Fig. 6. In the time-periodic regime this occurs for the discrete times $t_n = (n + 1/2)T_{level}$, $n = 1, 2, \dots$. Therefore, the t_n mark preferred values for the QP excitation time τ_c . In Fig. 8 the $1/t_n$ are marked as thin, horizontal lines $1/\tau_c$ jumps discontinuously between those values, with plateau-like behavior between the jumps. Which of the $1/t_n$ is realized for a particular level spacing Δ depends on the detailed non-linear dynamics of the system and can lead to resonance-like behavior, as seen in Fig. 8. For $n \rightarrow \infty$, τ_c diverges. Since the numerical time evolution is limited to finite times, we can resolve only finite n . For the initially self-trapped junction, one observes similar behavior (Fig. 9), however for substantially greater values of

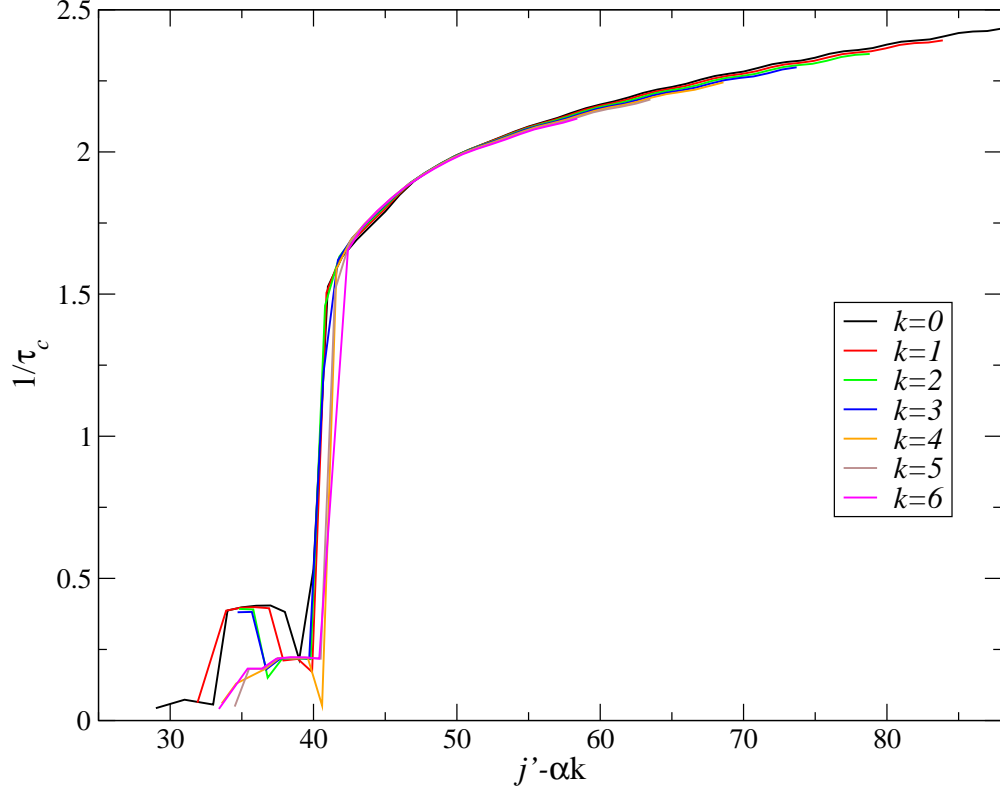


FIG. 12: Collapse of the $\tau_c^{-1}(j')$ curves of Fig. 11 by shifting $j' \rightarrow j' - \alpha k$ for different k . For the present parameters the coefficient $\alpha \approx 5.1$.

Δ , due to the substantially larger BEC oscillation frequency (compare Figs. 4 and 5).

The smallest value of the level spacing, Δ_{res} , for which a discrete $\tau_c = t_n$ is realized (resonance-like structures in Fig. 8) can be used to separate the regimes of continuous and discrete τ_c behavior. We find a linear increase of Δ_{res} with the QP-assisted Josephson tunneling amplitude j' , as seen in Fig. 10. In the regime below the line τ_c behaves continuously, above the line it takes discrete values. Note, that this “phase diagram” depends only weakly on the number of particles in the system.

In Fig. 11 we present the dependence of the inverse τ_c versus QP-assisted coupling j' for various values of the QP-BEC interaction k for an initially delocalized junction. One can see, when k is non-zero, it becomes more difficult to excite QPs, and increasing k results in larger values of τ_c . We attribute this remarkable behavior to the fact that k implies a level repulsion between the BEC levels $E_{c1,c2}$ and the QP level E_1 and, hence, inhibits QP excitations. At the resonance point, where E_{c2} and E_1 cross, the k -induced level repulsion is linear in k . Therefore, one expects τ_c to increase linearly with k . Indeed, the curves $\tau_c^{-1}(j')$

for different k collapse onto a single curve by shifting j' by a term linear in k , as shown in Fig. 12.

VI. CONCLUSIONS AND DISCUSSION

We studied in detail the non-equilibrium dynamics of a double-well Bose Josephson junction in two cases: the junction is initially delocalized, and the junction is initially self-trapped in a semiclassical meaning described in Ref. [23]. The non-equilibrium is caused by the abrupt switching on of the Josephson coupling between the well, which corresponds to the experimental situation [5]. We treat our system within Bogoliubov-Hartree-Fock first order approach and develop within it the non-equilibrium equations of motion for the condensate and QP parts of our Hamiltonian.

Our main finding is that the quasiparticle dynamics does not immediately set in at the time when the Josephson coupling is turned on, but after a certain period τ_c . At τ_c , QPs are excited in an avalanche manner due to fast quasiparticle oscillations between the discrete energy levels of the system. τ_c corresponds to a moment in time when the highest condensate eigenenergy is coincident with the eigenenergy of the first excited level. It depends on the system parameters in a complex way, including regimes of continuous and discrete behavior, which we have analyzed in the present work. The appearance of a regime with large, discrete τ_c explains the experimental finding that a junction can maintain undamped Josephson oscillations, although the barrier between the wells was ramped up in a sudden way [5].

We find furthermore that, when QP dynamics sets in, the junction inevitably switches to a π junction, a junction, whose time-dependent phase difference is equal to π when averaged over time. This is a necessary condition for sustaining fast Rabi-like oscillations between the QP levels. In the future we aim at studying how the non-equilibrium Josephson junction will equilibrate (if at all). This requires considering collisions between the quasiparticles in the full second order approximation.

Appendix: Particle and energy conservation

For any closed system the particle number and energy are conserved quantities. The particle number conservation arises as a consequence of the invariance of the Hamiltonian under global phase change. The mean particle number can be expressed in terms of the condensates wavefunctions and the statistical function, as follows

$$\langle N \rangle(t) = N_1 + N_2 + \sum_{n \neq 0} N_b^{(n)} = \sum_{\alpha=1,2} a_\alpha^*(t) a_\alpha(t) + \sum_{n \neq 0} \left[i F_{nn}^G(t, t) - \frac{1}{2} \right] \quad (74)$$

and it can be proven to be constant by making use of the equations of motion for a_α and F_{nn}^G . It is well known, that the exact solution of an isolated system excludes dissipation. One must therefore take care that the self-energies are derived within a conserving approximation (otherwise the non-physical dissipation can take place). If (like in our case) the self-energies \mathbf{S} and $\mathbf{\Sigma}$ are derived by means of a conserving approximation, for instance from a Luttinger-Ward functional [43, 44], the mean energy can be written as

$$\langle H \rangle = \langle H \rangle_{cond} + \langle H \rangle_{exc}, \quad (75)$$

and can be proven to be conserved. The energy of the condensate fraction is

$$\langle H \rangle_{cond}(t) = \frac{i}{2} \text{Tr} \left[\left(E_{\alpha\beta} \mathbb{1} + \frac{1}{2} \mathbf{S}_{\alpha\beta}^{HF}(t) \right) \mathbf{C}_{\beta\alpha}(t, t) \right] + \frac{1}{2} \text{Tr} \left[\int_{-\infty}^t d\bar{t} \gamma_{\alpha\gamma}(t, \bar{t}) \mathbf{C}_{\gamma\beta}(\bar{t}, t) \right], \quad (76)$$

and the energy of the QP excitations is

$$\begin{aligned} \langle H \rangle_{exc}(t) &= \frac{i}{2} \text{Tr} \left[\left(\epsilon_n \delta_{nm} \mathbb{1} + \frac{1}{2} \mathbf{\Sigma}_{nm}^{HF}(t) \right) \mathbf{F}_{mn}(t, t) \right] \\ &+ \frac{1}{2} \text{Tr} \left[\int_{-\infty}^t d\bar{t} (\mathbf{\Gamma}_{nm}(t, \bar{t}) \mathbf{F}_{mn}(\bar{t}, t) - \mathbf{\Pi}_{nm}(t, \bar{t}) \mathbf{A}_{mn}(\bar{t}, t)) \right] \\ &+ \frac{1}{2} \text{Tr} \left[\int_{-\infty}^t d\bar{t} (\mathbf{F}_{nm}(t, \bar{t}) \mathbf{\Gamma}_{mn}(\bar{t}, t) - \mathbf{A}_{nm}(t, \bar{t}) \mathbf{\Pi}_{mn}(\bar{t}, t)) \right]. \end{aligned} \quad (77)$$

Here again we sum over all indices appearing twice in every term. In the numerical solution of the time-dependent equations of motion the self-energies are calculated inherently in a self-consistent way, since in each time step of the numerical solution, the full solution of the previous step is used.

-
- [1] F. Dalfovo *et al.*, Rev. Mod. Phys. **71**, 463 (1999).
 - [2] A. J. Leggett, Rev. Mod. Phys. **73**, 307 (2001).
 - [3] M. Greiner *et al.*, Nature **415**, 39 (2002).
 - [4] M. Greiner *et al.*, Nature **419**, 51 (2002).
 - [5] M. Albiez *et al.*, Phys. Rev. Lett. **95**, 010402 (2005).
 - [6] S. Levy, E. Lahoud, I. Shomroni and J. Steinheuer, Nature **449**, 579 (2007).
 - [7] T. Salger, S. Kling, T. Hecking, C. Geckeler, L. Morales-Molina, and M. Weitz, Science **326**, 1241 (2009).
 - [8] C. Kollath, A. M. Läuchli, and E. Altman, Phys. Rev. Lett. **98**, 180601 (2007).
 - [9] H. U. R. Strand, M. Eckstein, and P. Werner, arXiv-cond-mat: 1405.6941 (2014).
 - [10] K. Sakmann, A. I. Streltsov, O. E. Alon, and L. S. Cederbaum, Phys. Rev. Lett. **103**, 220601 (2009).
 - [11] T. Kinoshita, T. Wenger, and D. S. Weiss, Nature **440**, 900 (2006).
 - [12] L. J. LeBlanc *et al.*, Phys. Rev. Lett. **106**, 025302 (2011).
 - [13] S. T. Beliaev, Soviet Phys. JETP **7**, 289 (1958).
 - [14] L. P. Kadanoff, and G. Baym, *Quantum Statistical Mechanics*, W. A. Benjamin, Inc., Menlo Park, California 1962.
 - [15] J. W. Kane, L. P. Kadanoff, J. Math. Phys. **6**, 1902 (1965).
 - [16] P. C. Hohenberg and P.C. Martin, Ann. Phys. (N. Y.) **34**, 291 (1965).
 - [17] A. Griffin, T. Nikuni, and E. Zaremba, *Bose-Condensed Gases at Finite Temperatures*, Cambridge University Press 2009.
 - [18] H. T. C. Stoof, in *Coherent Atomic Matter Waves*, Proceedings of the Les Houches Summer School Session 72, 1999, edited by R. Kaiser *et al.* (Springer-Verlag, Berlin, 2001).
 - [19] R. Baier and T. Stockamp, *Kinetic equations for Bose-Einstein condensates from the 2PI effective action*, arXiv:hep-ph/0412310 (2004).
 - [20] A. M. Rey, B. L. Hu, E. Calzetta, A. Roura, and C. W. Clark, Phys. Rev. A **69**, 033610 (2004).
 - [21] M. Trujillo-Martinez, A. Posazhennikova, and J. Kroha, Phys. Rev. Lett. **103**, 105302 (2009).
 - [22] This is exactly true if the left and right wells are separated.
 - [23] A. Smerzi, S. Fantoni, S. Giovanazzi, and S. R. Shenoy, Phys. Rev. Lett. **79**, 4950 (1997).

- [24] B. D. Josephson, Phys. Lett. **1**, 251 (1962).
- [25] A. Barone, G. Paterno, *Physics and Applications of the Josephson Effect*, John Wiley and Sons, New York (1982).
- [26] S. V. Pereverzev, A. Loshak, S. Backhaus, J. C. Davis, and R. E. Packard, Nature **388**, 449 (1997).
- [27] K. Sukhatme, Y. Mukharsky, T. Chui, and D. Pearson, Nature **411**, 280 (2001).
- [28] J. Javanainen, Phys. Rev. Lett. **57**, 3164 (1986).
- [29] M. W. Jack, M. J. Collett, and D. F. Walls, Phys. Rev. A **54**, R4625 (1996).
- [30] G. J. Milburn, J. Corney, E. M. Wright, and D. F. Walls, Phys. Rev. A **55**, 4318 (1997).
- [31] L. Radzihovsky and V. Gurarie, Phys. Rev. A **81**, 063609 (2010).
- [32] R. Gati and M. Oberthaler, J. Phys. B: At. Mol. Opt. Phys. **40**, R61 (2007).
- [33] T. Betz *et al.*, Phys. Rev. Lett. **106**, 020407 (2011).
- [34] F. S. Cataliotii *et al.*, Science **293**, 843 (2001).
- [35] I. Zapata, F. Sols, and A. J. Leggett, Phys. Rev. A **57**, R28 (1998).
- [36] I. Zapata, F. Sols, and A. J. Leggett, Phys. Rev. A **67**, 021603(R) (2003).
- [37] L. Pitaevskii and S. Stringari, Phys. Rev. Lett. **87**, 180402 (2001).
- [38] J. Esteve *et al.*, Nature (London) **455**, 1216 (2008).
- [39] H. T. C. Stoof, K. Gubbels, and D. B. M. Dickerscheid, *Ultracold Quantum Fields*, Chapt. 11.3.3, p. 246, (Springer-Verlag, Dordrecht, 2009).
- [40] M. Trujillo-Martinez, A. Posazhennikova, J. Kroha, to be published.
- [41] L. V. Keldysh, Sov. Phys. JETP **20**, 1018 (1965).
- [42] J. Rammer, *Quantum Field Theory of Non-equilibrium States*, Cambridge University Press 2007.
- [43] G. Baym and L. Kadanoff, Phys. Rev. **124**, 287 (1961).
- [44] G. Baym, Phys. Rev. **127**, 1391 (1962).